

Determination of the ionization and acceleration zones in a Stationary Plasma Thruster

N. Dorval, J. Bonnet, J.P. Marque, E. Rosencher
ONERA/DMPH, Chemin de la Hunière, 91761 Palaiseau (France)
dorval@onera.fr, jean.bonnet@onera.fr, marque@onera.fr, rosencher@onera.fr

S. Chable, F. Rogier
ONERA/DTIM, 2 avenue E. Belin, 31055
Toulouse (France)
chable@onera.fr, rogier@onera.fr

P. Lasgorceix
LAMO,
3 Avenue de la Recherche Scientifique, 45071,
Orléans Cedex 2 (France)

IEPC-01-21

A stationary plasma thruster is experimentally studied using different optical spectroscopies of xenon ions. Doppler shift in laser induced fluorescence is used for velocity determination while the ion density is determined by emission spectroscopy. These experiments show unambiguously that the ionization and the acceleration zones are spatially distinct inside the thruster channel. The results compare well with a stationary quasi neutral one-dimensional model.

Introduction

*Thanks to their high specific impulses and high thrust efficiency, Hall thruster or stationary plasma thrusters (SPT) are currently envisaged for commercial, extraplanetary and military space missions. These devices have been mostly developed by Russian teams in the early 1970s [1]. One of the main advantages of SPT compared to electrostatic ion thrusters is that the ion accelerating cathode is virtual, localized near the magnetic field maximum-where the electron mobility is decreased due to the electrons being trapped on Larmor orbits. Optical methods turned out to be superior to sampling ones-e.g. Langmuir probes- for a non-disturbing and sensitive analysis of plasma flows. Laser Induced Fluorescence (LIF) spectroscopy is well suited to probing species produced in SPT such as xenon ions, Xe^+ and measuring their velocities with both selectivity and high spatial resolution. This technique has already been used to investigate Hall type thrusters. Let's cite

here the works of Manzella [2] and of Hargus and Cappelli [3]. Here we present LIF and plasma emission experiments results inside and outside the channel of a SPT-100. We report on the measured axial profiles of $Xe^+ 5d \{ \{ \} 4 \{ \} \} 7/2$ axial velocity and of $Xe^+ 6p \{ \{ \} 3 \{ \} \} 5/2$ emission at 541.9 nm. We unambiguously demonstrate that ionisation and acceleration occur in two different zones of the SPT. Then, we show that the experimental results agree satisfactorily well with a simple heuristic one-dimensional computational model.

Experimental results

The experiment took place in the "PIVOINE" facility of CNRS with the SPT 100-ML provided by SNECMA. This facility and the SPT 100-ML are described in details in ref [4]. The test facility consists in a vacuum chamber (2.2 m in diameter, 5 meter in length) with a cryogenic pumping system (pumping speed of 45 000 l/s). The thruster is fed with 5 mg s^{-1} of xenon (99.9995% pure) through the anode which yields a tank pressure of 2.7×10^{-5} mbar. It operates

* Copyright @2001 by the Electric Rocket Propulsion Society. All rights reserved

under the following conditions: discharge voltage=300V, discharge current= 4.25 A, magnetic coil current=4.5 A. Under these conditions, the thruster is working in a fluctuating current [4]. Measurement is performed at several axial locations from inside to outside the channel with a minimum step of 0.5 mm in the vicinity of the exit plane. Velocity is measured with a precision lying between $\pm 100 \text{ ms}^{-1}$ to $\pm 800 \text{ ms}^{-1}$. (The worst values are due to a significant broadening of the spectrum within a thin layer upstream the exit plane). Negative position $z < 0$. Figure 1 shows the recorded excitation spectra of Xe^+ from 2 to 25 mm downstream from the exit plane of the channel, together with the Xe^+ spectrum *simultaneously* measured in the zero-velocity reference plasma source (in dotted line).

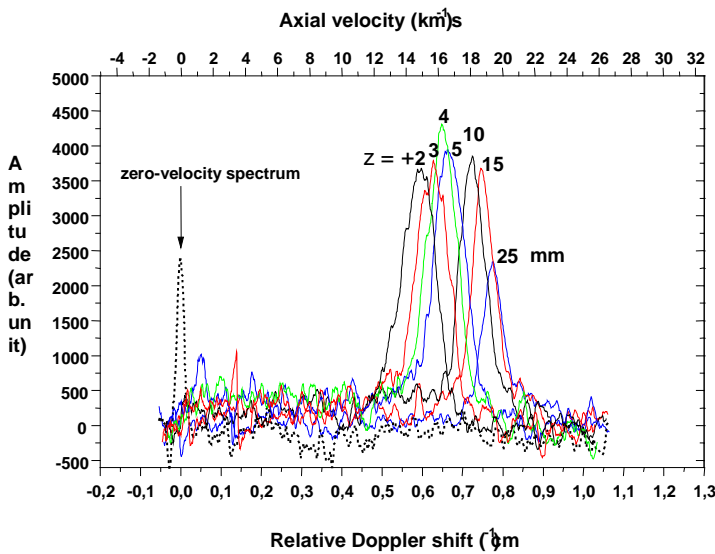


Figure 1

We clearly see the variation of the Doppler shift as well as of the width of the spectrum as a function of the axial location. Going inside the channel (i.e. +2 to -1 mm), one observes a progressive broadening of the spectra which is clearly seen on the normalized curves of Figure 2. It is worth noting that an almost twofold broadening of the spectrum occurs within 1.5 cm in the zone located between 0.5 and 2 mm inside the channel which affects strongly the precision of velocity measurement *i.e.* from ± 100 to 800 ms^{-1} . Also, the signal to noise ratio drops by a factor 3.

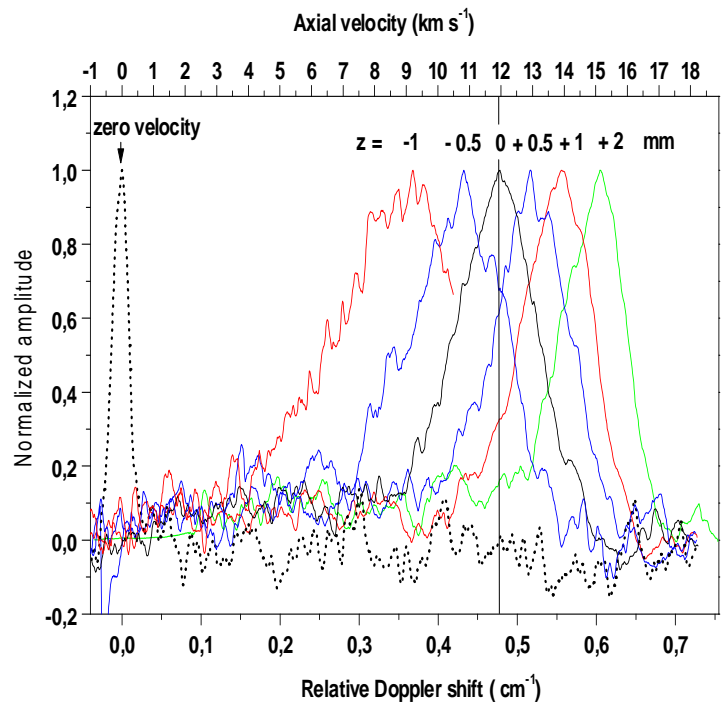


Figure 2

There is also the appearance of evenly spaced peaks in the spectrum (500 – 700 MHz) clearly seen in Figure 3.

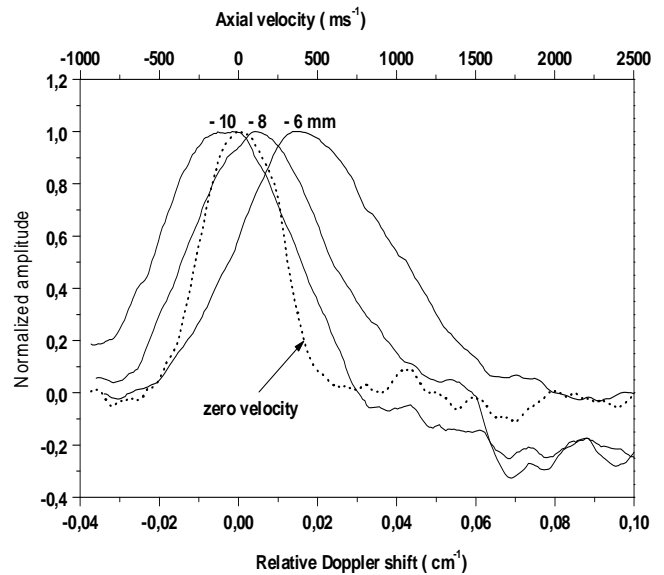


Figure 3

This striking change is likely to arise from plasma oscillations or instabilities but it has to be asserted by spectral simulation which could account for such effects. Finally, deeper inside the channel (see Figure 4), the Doppler shift vanishes, showing that ions are not yet accelerated and the spectrum width narrows to

a minimum value of 1.3 GHz (though it is always wider than the one recorded simultaneously in the microwave plasma in dotted line i.e. FWHM of ~700 MHz).

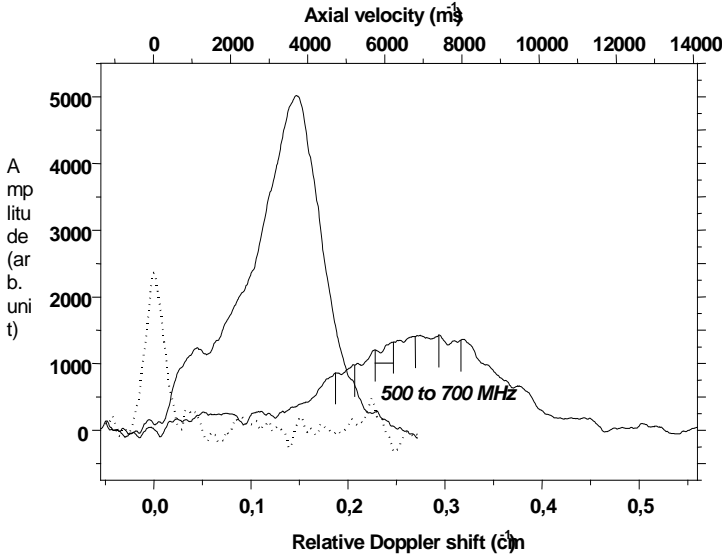


Figure 4

The interpretation of the spectrum shape and its exploitation to infer additional data such as velocity dispersion (or kinetic temperature), require the simulation of the hyperfine, isotopic and (possibly) Zeeman structures of the transition $5d[4]_{7/2}-6p[3]_{5/2}$ of Xe^+ , which will be done in a forthcoming publication. Figure 5 shows the spatial evolution of the ion velocity deduced from the Doppler shift measurements. One clearly observes that most of the acceleration (>80%) occurs from -2.5 cm to $+2.5$ cm. Moreover, in accordance with Hargus and Cappelli's results, a significant portion of the ion acceleration is obtained outside the SPT channel, i.e. away from the magnetic field maximum. This will be discussed later. Using the same detection apparatus, we have measured the 541.9 nm $Xe^+ 6p[3]_{5/2}$ fluorescence light spontaneously emitted by the plasma in the same working conditions. We assume that the quantity of 541.9 nm light emitted by the $(Xe^+)^*$ metastable ions is proportional to the plasma density.

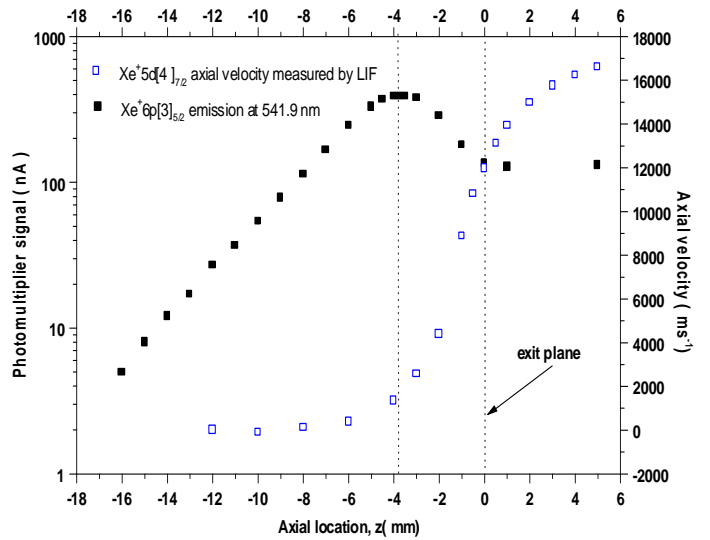


Figure 5

Figure 6 shows the measured signal together with the ion velocity distribution of Figure 5.

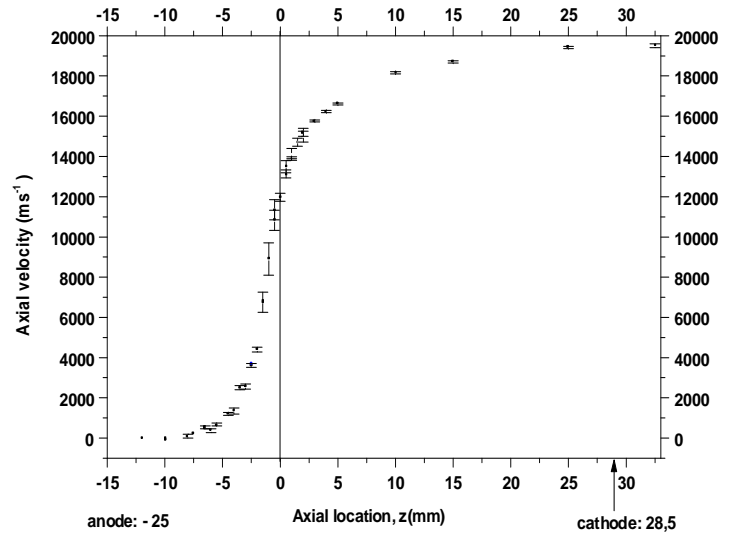


Figure 6

This figure confirms the main mechanism at stake in the SPT channel in nominal thrust conditions. The maximum plasma density is situated in a *ionisation region* which, by definition, is the region where the ion density and ionisation rate are (almost simultaneously) maximum. For nominal working conditions, this ionisation zone is situated inside the SPT channel. The ions are then accelerated by the electric field which increases dramatically in the region of maximum magnetic field in order to compensate the decrease of the mobility of the electrons trapped on their Larmor orbits. This will be

confirmed by the numerical model below. Let us note finally the exponential decrease of the plasma density towards the anode electrode. In order to have a closer look at this *acceleration zone*, we first calculate the kinetic energy E_c of the Xe^+ ions from data of Figure 5. The electric field is then determined by the spatial derivation of this kinetic energy dE_c/dz . Let us note that this latter calculation is valid for two conditions:

- the ion transport is ballistic (which is an excellent approximation),
- the Doppler lineshape is not too disturbed so that the maximum of the lineshape still reflects the ion mean velocity.

The results are shown in figure 7.

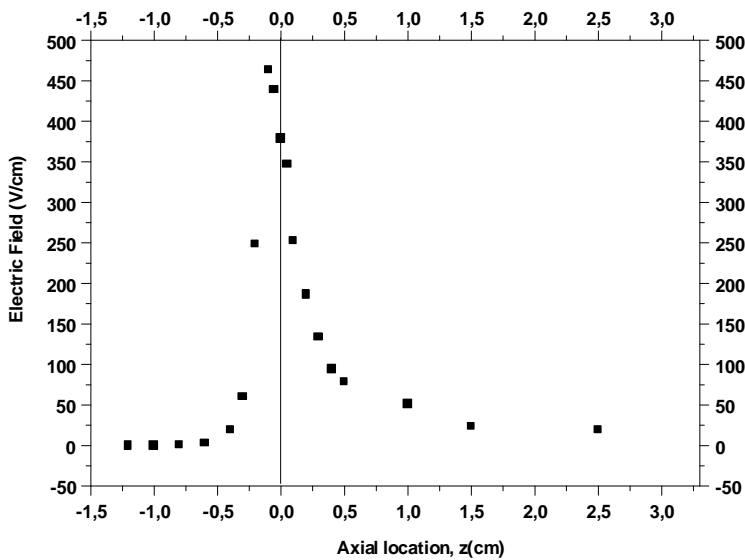


Figure 7

The acceleration zone is clearly peaked in the channel near the thruster output, i.e. at the magnetic field maximum, This acceleration zone is rather thin since the full width at half maximum (FWHM) is less than 2 mm wide but it extends rather deeply in the plume since significant electric field (50 V/cm) are still reigning 10 mm away from the SPT exit.

Numerical model

Analysis of our experimental results is now performed with the support of a plasma simulation which is described below . The basis of this approach is to use a simple one-dimensional model in order to

specifically address the main points covered by our experiments:

- the acceleration outside the channel and
- the two different zones (i.e. ionization and acceleration) in the channel.

In order to best understand the work conditions of the SPT a stationary quasi neutral one dimensional numerical model based on the physical modelling proposed by Boeuf and Garrigues [] has been written. This numerical code aim to help to analyse experimental results and to study the effect of various physical parameters on the discharge current. Obviously, plasma oscillations are not predicted but numerical comparison show a good agreement with averaged time solution. In order to confirm and improve qualitative results obtained by the one dimensional modelling. A 2D unsteady numerical code using Particle In Cell methods based on different approaches developped previously (see for example Boyd [10], Martine-Sanchez [11] or Boeuf [12], [13] is in progress. The main assumptions of the one dimension modelling are the following: the electrons are approximated by a Maxwellian fluid, the heavy particles are ballistic, the magnetic field (supposed only radial) is only due to the external magnetic coils while the one induced from the current through the SPT is neglected (i.e. not selfconsistent), the electronic mobility includes the electrons wall collisions, ions are not sensitive to the magnetic field and the neutral Xe velocity is spatially constant. The model is extended outside the channel to the cathode taking into account the magnetic field distribution outside the channel. The electric potential is supposed to be equal to 0 at the cathode. v_0 is the neutral velocity. k_i is the ionisation rate which depends on the mean electronic energy ϵ . It is deduced from the Bœuf-Pitchford model [5]: a steady state mean energy equation is considered. Only single ionisation is included in the model. A non trivial point consists in the treatment of the plasma interaction with the insulator wall. Since an electron impacting a solid surface may be scattered back, a proportion of its energy is transferred to secondary electrons. This mechanism represents a significant energy loss at temperatures around 30eV for which the emission coefficient for secondary electrons approaches 1 [5]. Garrigues [6] takes into account the electron-wall interactions by including an electron-wall momentum exchange frequency α and an electron-wall energy

exchange frequency which takes the simple form: $\alpha \exp(-\frac{U}{\epsilon})$ where U is a constant Debye sheath

voltage and ϵ is the electron mean energy. This expression is deduced from the assumption of an electron Boltzmann distribution. α is proportional to the electron thermal velocity and inversely proportional to the distance between the two radius. The results obtained are not sensitive to the variation of the wall potential. Outside the channel, in order to avoid a non physical singularity in the energy profile, the wall-electron interactions are smoothly faded to zero at 1.5 cm from the exhaust. This fading term allows the electron to drift away from this region where the magnetic field is still large enough to trap them on Larmor orbits. It is most likely that this heuristic term stems physically from 2D effects which are not described by this simple approach (radial gradient of the magnetic and electric fields). Other approaches have been tried such as introducing a Bohm diffusion term [7, 8] to explain the presence of anomalous cross-field electron mobility but the results were not convincing. This fading term will be investigated in forthcoming publications by 2D simulations. The electron density is deduced from the quasi-neutrality condition. The electron momentum equation is supposed to take the simple form : $v_e = -\mu E$, where μ is the classical electron mobility in a transverse magnetic field[8] :

$$\mu(z) = \frac{e}{m_e \nu(z)} \frac{1}{1 + (\omega_B^2 / \nu^2)(z)}$$

where ω_B is the cyclotron frequency. The collision frequency ν is given by $\nu(z) = \nu_m(z) + \nu_w$ which takes into account the electron-wall interactions $\nu_w = 0.2 \cdot 10^7 \text{ cm}^{-1}$ and the electron-neutral collisions $\nu_m(z) = k_m n_0(z)$ with $k_m = 2.5 \cdot 10^{-7} \text{ cm}^3 \cdot \text{s}^{-1}$. The displacement current is neglected and the electric field is resolved using the current continuity. We refer to Ref [6] for more details.

The calculation is over identical four hundred cells. The numerical simulation takes one minute on a 440 MHz Sun workstation.

Results and discussion

We discuss now the resulting axial profiles of the plasma parameters. We take the physical parameters of SPT-100 ML as :

- column voltage of 300 V
- a mass flow rate of 5 mg/s

a magnetic field distribution shown in Figure 8 experimentally determined by Hall probes .

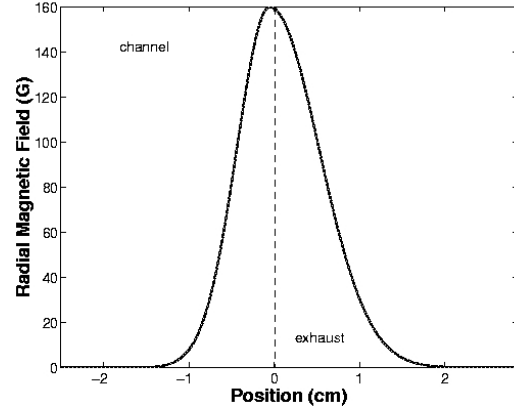


Figure 8

The peak is obtained close to the channel exit and decreases outside the channel. For some values of the applied voltage ($>400 \text{ V}$ see Ref [4]), the SPT is known to display oscillations. We have checked that, for cases with oscillations, the time averaged profiles of our stationary model are similar to the profiles of the non stationary model . This justifies the use of our stationary approach which leads to far smaller computational time than the non stationary one. In Figure 9 ,it appears that the electric field maximum occurs inside the channel close to the exit plane where the radial magnetic field reaches its maximum value: This zone, named the “acceleration zone”, is the zone where the positive ions are accelerated and extracted from the plasma.

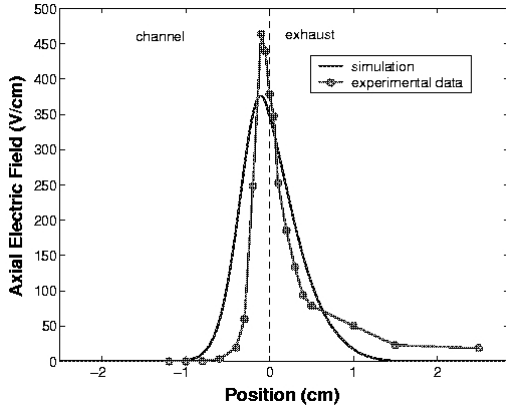


Figure 9

This is indeed the basic principle of SPT in action since the electric field in the large magnetic field region increases in order to compensate for the low electron conductivity and to ensure current continuity. In other words, the electric field is roughly inversely proportional to the mobility, i.e. proportional to the square of the magnetic field through equation. In Figure 10, the electron mean energy is found to be maximum close to the exit channel and decreases in the low electric field regions.

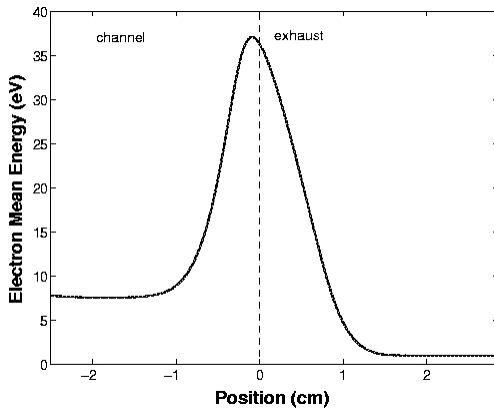


Figure 10

Outside the channel, it remains constant to a value which can be taken as a parameter. We have chosen a value of 1 eV in order to prevent Xe numerical ionization outside the channel by the Maxwellian tail of the electron distribution. Indeed, taking a larger limit condition of 10 eV yields numerical ionisation of Xe which is not observed experimentally. Figure 11 shows that the plasma density reaches a value of $1.2 \cdot 10^{12} \text{ cm}^{-3}$ at a distance of 0.5 cm inside the channel.

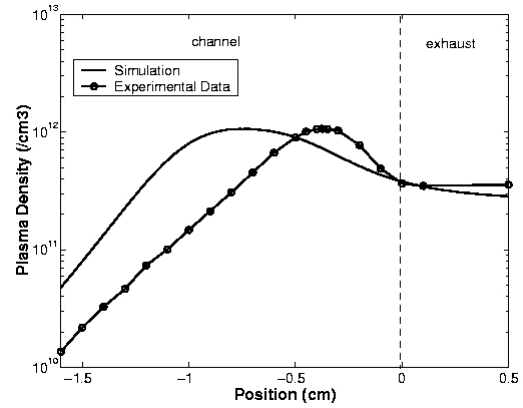


Figure 11

Outside the channel, the ion density slightly decreases because it is just accelerated by the electric field : they are not collisional and become ballistic. This is in contrast with Figure 12 where the neutral density is shown to be constant from the anode to 1,75 cm from the exit and decreases to reach about 10% of its anode value due to ionisation.

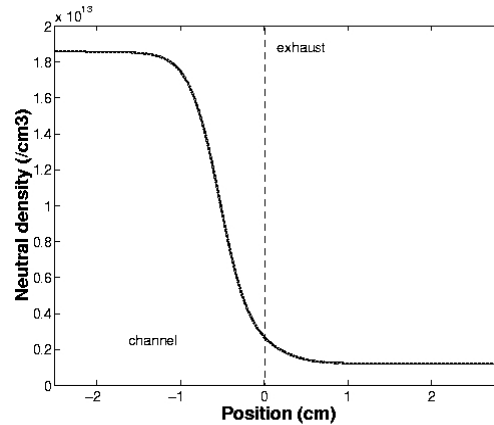


Figure 12

The transition region where most of the ionization takes place is also named “production zone” or “ionization zone”.

Figure 13 compares the axial ion velocity determined by the LIF measurements and the result of the model.

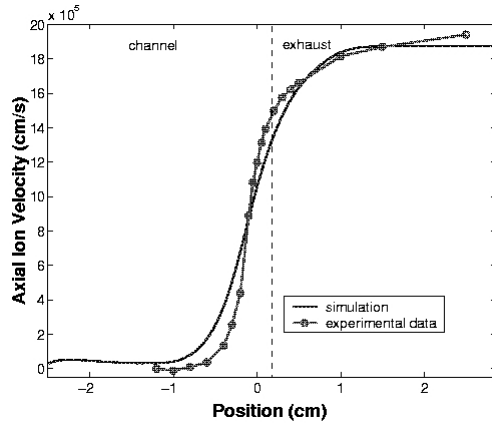


Figure 13

In spite of the simplicity of our heuristic model and the two dimensional effects which take place inside and outside the channel – the magnetic field lines are strongly curved – the agreement is rather satisfactory. The ion velocity increases to reach in the exhaust about 12000 m.s^{-1} . Outside the channel, it is almost constant and equal 19500 m.s^{-1} . In quadratic norm, there is an error of 7% between the experiment and the model. Finally, Figure 11 shows the calculated plasma density. This overall profile agrees rather well with the experimental axial profile of the $\text{Xe}^+ 6p[3]_{5/2}$ plasma emission of Figure 6 (shown again in Figure 11): there is effectively an exponential increase of the plasma density from the anode and the plasma density varies only slightly in the acceleration zone. However, there is an important discrepancy between the experimental curve and the numerical model output. For instance, in the exponential increase region (between 2 cm and 0.5 cm from the exhaust), the theoretical gradient is 25% larger than the experimental one. It is thus clear that physical phenomena are still poorly understood in this region. Finally, the ion current is calculated to be about 3.85 A at the cathode. It corresponds to a thrust of about 0.094 N and a specific impulse of 1913 s. This is in good agreement with experimental results (the thrust calculated from the experimental axial ion velocity is 0.098 N).

Conclusions

Optical spectroscopy measurements have unambiguously displayed two different regions in the SPT thruster:

- an ionization zone where most of the plasma is created and where the $\text{Xe}^+ 6p[3]_{5/2}$ plasma emission is maximum.

In this region, the magnetic field is small, the electron mobility is thus high and correlatively the electric field is small. The electron energy is then small enough to meet the maximum of the Xe ionization yield.

- an acceleration zone where the $5d \ ^4F_{5/2} - 6p \ ^4D_{5/2}$ singly ionised xenon transition is maximum.

In this region, the magnetic field is high, the electron mobility is low, the electric field is high for achieving current continuity and, consequently, the ions are highly accelerated. The HWHM of this high field region profile is extremely thin, i.e. in the 2 mm. However, an important part of the ion acceleration takes place outside the SPT channel, where the magnetic field is still high. Because of the radial component of this magnetic field, the acceleration is divergent, which is confirmed by experiments. In order to reduce the plume divergence, a good idea is to improve the magnetic field topology at the exit part of accelerating[9], which calls for a real 2D model. The one-dimensional quasi-neutral stationary model has been shown to be very useful in analysing the physics of SPT operation thanks to a short time of calculation. In spite of the simplicity of the model, the numerical results are in good agreement with the experimental data. An important ingredient for this successful agreement is the introduction of an heuristic fading function of the wall-electron interactions outside the SPT channel. This approximation will be validated by future 2D simulations.

Acknowledgement: The authors are indebted to CNES and the Conseil de l'Ile de France for financial support as well as to Serge Larigaldie from ONERA and Michel Lyszyk of SNECMA for fruitful discussions.

References

- [1] A. I. Morozov, Y. V. Esipchuk, G. N. Tilinin, A. V. Trofimov, Y. A. Sharov, and G. Ya. Shshepkin, "Plasma accelerator with closed electron drift and extended acceleration zone," *Soviet Physics Technical Physics*, vol. 17, n°1, p.38, 1972.

- [2] D. H. Manzella, "Stationary Plasma Thruster Ion Velocity Distribution," presented at the *30th AIAA/ASME/ASEE joint Propulsion Conference* June 27-29, 1994, Indianapolis, IN (USA), 1994.
- [3] W. A. J. Hargus and M. A. Cappelli, "Interior and Exterior Laser-Induced Fluorescence and Plasma Potential measurements on a laboratory Hall thruster," presented at the *35th AIAA/ASME/ASEE Joint Propulsion Conference* 20-24 June (1994), Los Angeles, CAL (USA), 1999.
- [4] M. Lyszyk, A. Cadiou, M. Dudeck, and J. P. Marque, "Recent results on plasma thrusters in France," presented at *3rd International Conference on Spacecraft Propulsion ICSP*, Cannes (France), 2000.
- [9] M. Day, V. Kim, V. Kozlov, A. Lazurenko, G. Popov, and A. Skrylnikov, "Investigation of the Possibility to Reduce SPT Plume Divergence by Optimization of the Magnetic Field Topology in the Accelerating Channel," presented at *25th IEPC*,
- [10] D.B. Van Gilder and I.D. Boyd, *34th AIAA Joint Propulsion Conference*, paper AIAA-98-3797, Cleveland, 1998.
- [11] J.M. Fife, M. Matinez-Sanchez and J. Szabo, "A Numerical Study of Low-Frequency Discharge Oscillations in Hall Thrusters," presented at the *33rd AIAA Joint Propulsion Conference*, Seattle, 1997.
- [12] J. Bareilles, L. Garrigues and J.P. Bœuf, "Modeling of the Plume of a Stationary Thruster", presented at the *3rd International conference on Spacecraft Propulsion*, Cannes, 2000.
- [13] L. Garrigues, A. Heron, J.C. Adam and J.P. Bœuf, "Hybrid and Particle-In-Cell Models in a Stationary Plasma Thruster, *Plasma Source Sci. Technol.*, 9, 219-226, 2000.
- [5] J. P. Boeuf, L. Garrigues and L. C. Pitchford, "Electron Kinetics and Applications of Glow Discharges", edited by U. Kortshagen and L. Tsendin, Plenum Press, New-York, 1998
- [6] L. Garrigues and J. P. Boeuf, "Low frequency oscillations in a stationary plasma thruster," *Journal of Applied Physics*, vol. 84, pp. 3541-3554, 1998.
- [7] N. B. Meezan, W. A. Hargus, and M. A. Cappelli, "Anomalous electron mobility in a coaxial Hall discharge plasma," *Physical Review E*, vol. 63, 2001.
- [8] F. Chen, *Introduction to Plasma Physics and Controlled Fusion*. New York: Plenum Press, 1984.